

Vasculature and flow in microfluidic systems Kramer, B.

Citation

Kramer, B. (2025, October 23). Vasculature and flow in microfluidic systems. Retrieved from https://hdl.handle.net/1887/4279472

Version: Publisher's Version

Licence agreement concerning inclusion of doctoral

License: thesis in the Institutional Repository of the University

of Leiden

Downloaded from: https://hdl.handle.net/1887/4279472

Note: To cite this publication please use the final published version (if applicable).

Chapter 5

A robust and high-throughput approach for the quantification of three-dimensional vascular beds

Bart Kramer, Marianne Swart, Thomas Olivier, Lenie van den Broek

In preparation for publication



5

Abstract

Angiogenesis, the formation of new blood vessels from pre-existing ones, is a complex biological process integral to many physiological and pathological processes. It involves intricate interactions between various cell types, notably endothelial cells and pericytes. In this study, we present an innovative method for studying and quantifying angiogenesis in vitro, leveraging the advantages of high-throughput three-dimensional (3D) imaging. Utilizing the OrganoPlate Graft, we created a controlled environment for vascular bed formation, and subsequently introduced pericytes into the model system to better understand their role in angiogenesis. The application of a fluorescent confocal method for 3D imaging allowed for a more detailed and comprehensive understanding of the vascular bed. Our results demonstrate that 3D analysis is complementary to 2D analysis, but may provide a more precise measurement, offering a robust and efficient approach for studying angiogenesis. This innovative methodology could potentially expedite the development of targeted therapies for diseases characterized by abnormal angiogenesis.

Introduction

The vascular network is a vital part of the circulatory system responsible for providing the body with necessary nutrients, oxygen, and hormones. It also plays an important role in removal of metabolic waste, maintenance of blood pressure, thermoregulation, and moreover, it is involved heavily in the immune response. Endothelial cells and pericytes are important cell types that play key roles in the maintenance of vascular homeostasis. Endothelial cells form the innermost layer of the vascular wall, and they are responsible for controlling the passage of substances, such as ions and small molecules, into and out of the vascular lumen. Pericytes are found in the basement membrane of the vascular wall and are involved in the regulation of vascular formation, maturation, and function. In addition, pericytes play an important role in vessel stability, repair and regulating angiogenesis. 4,5

Angiogenesis is the process of forming new blood vessels from pre-existing ones. It plays an important role in many physiological and pathological processes, such as wound healing, tumor growth and metastasis.^{6,7} The interaction between endothelial cells and pericytes is essential for proper vessel formation and stabilization.(Ribatti, Nico, and Crivellato 2011) For example, when endothelial sprouts form during angiogenesis, pericytes migrate towards them and attach themselves to the growing vessel wall. Without pericytes, endothelial sprouts are unstable and prone to collapse, which can lead to impaired blood flow and tissue damage.8 Although in vivo model systems for angiogenesis have been used for decades,9 there is a growing need for accurate in vitro model systems to study this process. In vitro models are generally more easily controlled, less expensive and more ethically responsible than the use of in vivo models.¹⁰ The gold standard in vitro assays, like spheroid-based outgrowth and 2D vessel models, offer precise platforms for studying angiogenesis. Spheroid assays mimic early angiogenesis by analyzing tip cell formation, while 2D models focus on endothelial cell migration and tube formation.^{11,12}

128 | Robust and high-throughput quantification of 3D vascular beds

Studying these complex biological processes, particularly angiogenesis, necessitates imaging methods that can accurately capture the three-dimensional structure of the vascular bed. Conventional two-dimensional (2D) imaging techniques, like Computed Tomography (CT) or Magnetic Resonance Imaging (MRI), often fall short due to limited spatial resolution and difficulties in adapting these techniques to in vitro models.^{13–15} These challenges, compounded by the complexity of multiple cell layers and various cell types, have prompted a shift towards three-dimensional (3D) imaging techniques.

The application of 3D imaging promises significant advantages, notably superior spatial resolution, that allow for a more detailed and comprehensive understanding of the vascular bed. Unlike 2D imaging, 3D imaging enables the visualization of structures in their natural context, enhancing the representation of cell-to-cell interactions, morphologies, and positions. These attributes make 3D imaging indispensable when investigating complex processes like angiogenesis and the precise roles played by endothelial cells and pericytes.

In this study, we investigated a method that capitalizes on the advantages of 3D imaging and quantification for studying in vitro vascular beds in high-throughput fashion. Building upon our previously optimized angiogenesis assay using a microfluidic device, ^{16,17} our approach incorporates the application of a fluorescent confocal method and subsequent analysis of the 3D images. This approach was compared with a more traditional Z-projection imaging quantification method, to identify the potential advantages of 3D quantification.

With the developed methods, the enrichment of our model system was investigated by introducing pericytes, alongside the endothelial cells, to better understand their roles and interactions in angiogenesis. By enhancing the spatial resolution of our imaging and expanding our cellular scope, we anticipate gaining a more comprehensive understanding of the complexities involved in blood vessel formation. Ultimately, this knowledge could expedite the development of targeted therapies for diseases characterized by abnormal angiogenesis.

Materials and methods

Cell culture

Primary Human Umbilical Vein Endothelial Cells (HUVECs, Lonza C2915AS) were cultured in T-75 Flasks (Corning, #734–2705) in MV2 (PromoCell, #C-22121) supplemented with 1% penicillin/streptomycin (Sigma, #P4333) and used at maximum passage 5 for experiments. Cells were cryopreserved by dissociation from the flasks with Trypsin/EDTA solution 0.25 mg/mL (Lonza CC-5012), counted and cryopreserved in a solution of 50% Fetal Calf Serum (FCS, Gibco, cat# A13450), 40% MV2 medium and 10% Dimethyl Sulfoxide (DMSO, Sigma, cat# D8418). For experiments, HUVECs were seeded in the microfluidic plate immediately after thawing a cryopreserved vial. Human Primary Brain Vascular Pericytes (Sciencell, cat# 1200) were expanded in Poly-L-Lysine (AMSbio Cultrex, cat# 3438-100-01) coated T-75 flasks in Pericyte medium (Sciencell, cat# 1201) and used at maximum passage 4 for experiments. Cells were cryopreserved by dissociation from the flasks with Trypsin/EDTA solution 0.25 mg/mL (Lonza CC-5012) and counted before using them for experiments.

Microfluidic Device Culture

Microfluidic culture was performed using the OrganoPlate Graft (MIMETAS). The microfluidics are patterned under a 384 wells industry standard titer plate divided in 64 microfluidic chips (Figure 1A). Each chip consists of two perfusion channels and a center gel channel (the graft chamber). The graft chamber is connected directly to the well above it, allowing for the addition of a small tissue or growth factors. 2.3 μ L of hydrogel composed of 4 mg/mL Collagen I (AMSbio Cultrex 3D Collagen I Rat Tail, 5 mg/ml, #3447–020-01), 100 mM HEPES (Life Technologies, #15,630–122), and 3.7 mg/ml NaHCO3 (Sigma, #S5761) was dispensed in the gel inlet and incubated 15 min at 37 °C. 1.5 μ L of endothelial cell suspension (or coculture suspension) was seeded in a density of 1×10 7 of cells/mL in the inlets of the perfusion channels (Figure 1B, well A1 and A3). In the co-culture conditions,

cells were loaded in a 1:19 ratio (pericyte:HUVEC). For the pericyte monoculture condition the seeding density was 4.5×10^6 cells/mL. After cell loading, the device was transferred to an incubator (37 °C and 5% CO₂) to allow for cell attachment over 2.5 hours. After cell attachment, 50 μ L of medium was added to the perfusion outlets and on top of the graft chamber, HBSS was removed from the gel inlets and the plates were placed on an interval rocker platform to ensure constant perfusion (OrganoFlow; MIMETAS, Leiden, The Netherlands). Medium was changed in all wells every 2-3 days.

When confluent endothelial vessels formed in the perfusion channels, sprouting was triggered by using an angiogenic cocktail consisting of 50 ng/mL vascular endothelial growth factor (VEGF, PeproTech, cat# 100-20), 500 nM Sphingosine 1-phosphate (S1P, Sigma-Aldrich, cat # 73914), 20 ng/mL Phorbol 12-myristate 13-acetate (PMA, Sigma-Aldrich, cat# P1585) and 20 ng/mL basic fibroblast growth factor (bFGF, PeproTech, cat# 100-18B). This cocktail was added to the medium on top of the graft chamber (Figure 1A, well B2) and the cells were allowed to sprout towards the center of the gel chamber up to 96 hours.

Fixation

HUVEC (+ pericytes) vessels and sprouts were fixated using 3.7% formaldehyde (Sigma, 252,549) in HBSS (Sigma H6648) for 15 min, washed twice with HBSS for 5 min and stored with 50ul HBSS per well at room temperature until immunofluorescent staining.

Perfusion assay

Fluorescein isothiocyanate (FITC)-dextran or Tetramethylrhodamine (TRITC)-dextran 150-155 kDa (Sigma-Aldrich, cat46946 or T1287) was used to visualize the perfusion of the vessels. 0.5 mg/mL FICT- or TRITC- dextran in medium was added in a volume of 20 and 40 μ L in the left perfusion inlet and outlet. 20 μ L of media was placed on top of the graft chamber, gel inlet, right perfusion inlet and outlet. Time-lapse images were taken every two minutes (up till 20 minutes) with the

ImageXpress Micro Confocal High-Content Imaging System (Molecular devices). Visualization of the images was done in ImageJ (Fiji).

Immunostaining

Staining, Cultures were washed with washing solution containing 4% Fetal Calf Serum (FCS) (Gibco, cat# A13450) in PBS (Gibco, cat# 70,013,065) for 5 min and permeabilized with 0.3% Triton X-100 (Sigma, T8787) in PBS for 10 min. After permeabilization, the cells were washed with washing solution for 5 min before the blocking buffer, containing 2% FCS, 2% BSA (Sigma, cat# A2153), and 0.1% Tween20 (Sigma, cat# P9616) in PBS, was added for 50 min. After blocking, the cells were immediately incubated for 2 h with a primary antibody in blocking solution, washed two times for 3 min with washing solution and incubated with a secondary antibody in blocking solution, including a nuclear stain, for 30 min. Primary antibodies used were: Rabbit anti-human VE-Cadherin 1:1000 (Abcam, Ab33168), Mouse anti-human αSMA 1:100 (Sigma, A2547), Rabbit antihuman PDGFR-beta 1:180 (Abcam ab32570), Mouse anti-human CD31 (1:50; Agilent M082301-2). Secondary antibodies used were: Goat-anti-Mouse IgG-Alexa 647 (1:250, Life Technologies) Goat-anti-Mouse IgG-Alexa 488 (1:250, Life Technologies), Goat-anti-Rabbit IgG-Alexa 488 (1:250, Life Technologies), Goatanti-

Rabbit IgG-Alexa 647 (1:250, Life Technologies). For direct stains, Lectin 1:100 (Sigma L9006) and Actin, 2 drops per mL, (Life Technologies R37110) were used. For nuclear staining Hoechst 33342 (Thermo Fisher Scientific H3570) 1:2000 was used.

Sprouting quantification

Nuclei quantification

Images of the Hoechst signal were acquired with the ImageXpress Micro Confocal High-Content Imaging System (Molecular Devices) and a maximum-projection was saved. Images were loaded in Fiji (ImageJ) and the number of nuclei from the images was extracted by thresholding the image and the 'analyze particles' function. Visualization of the data points was performed in GraphPad (Prism).

3-dimensional vascular bed quantification

Images were acquired with the ImageXpress Micro Confocal High-Content Imaging System (Molecular Devices). 55-70 images were acquired per chip from the middle region of the graft chamber. The quantification process is depicted in Figure 3B. Quantification was performed with the MetaXpress software (Molecular Devices). Gaussian blurs were performed to subtract background. Subsequently, objects were identified using the build-in neurite outgrowth module. With a filter mask, disconnected fragments were filtered out. The objects that were detected in each slide were connected via the connect by the maximum replacement feature. This feature connects the found objects based on the distance between them. Subsequent analysis was done in JMP (SAS institute) to generate summery values of the quantified sprouting segments. Nuclei counting was performed in ImageJ (FIJI) with the analyze particles tool. Visualization of the data points and statistical analysis was performed in GraphPad (Prism V9).

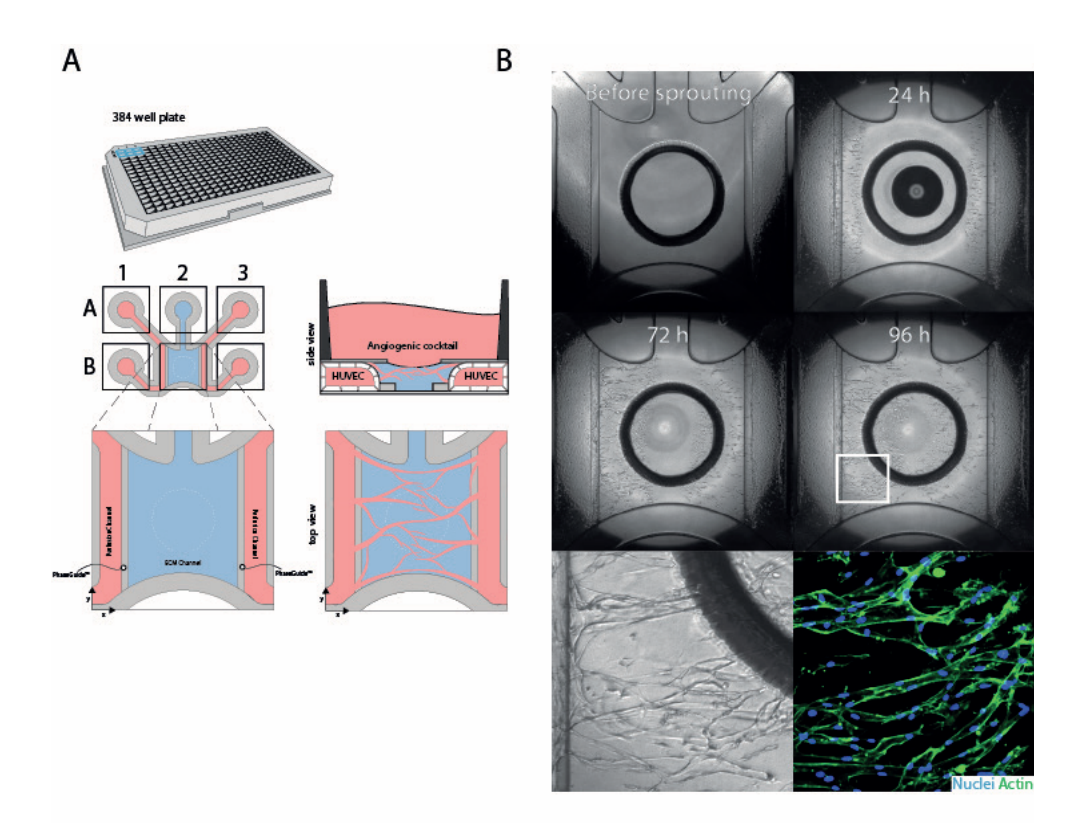
Results

Vascular bed formation in a 3D microenvironment

The microfluidic platform used in this study (OrganoPlate Graft) is based on a 384 wells industry standard titer plate divided in 64 microfluidic chips (Figure 1A). Human Umbilical Vein Endothelial Cells (HUVECs) were loaded on both sides of a collagen hydrogel and formed a tubular structure over time. Subsequently, angiogenesis was initiated towards the middle of the chip by addition of an angiogenic cocktail, where sprouts from both sides meet each other. Over 96 hours, a vascular bed formed in the middle 'graft chamber' of the chip (Figure 1A, well B2). To prove the perfusability of the formed vascular bed, a fluorescent dextran molecule was perfused through the left lateral HUVEC tubule. A fluorescent signal in the graft chamber was observed directly after addition of the dye (Figure 1C, middle panel), indicating that the formed sprouts were perfusable. After 20 minutes, the dye retained in the vessels, indicating that the formed vessels have a high barrier integrity (Figure 1C, right panel). In some cases, the dye reached the right lateral HUVEC tubule, proving a connection between the sprouts that formed from both HUVEC lateral vessels.

Development of the HUVEC/Pericyte co-culture

To investigate the effect of pericytes on endothelial cells in our microfluidic system, HUVECs and primary pericytes were co-seeded in the lateral channels and applied the angiogenic cocktail to the graft well. Vascular bed formation was observed, and the culture was characterized to investigate the position of the pericytes. HUVEC monoculture was positive for the adherence junction markers CD31 (also known as PECAM-1) and VE-cadherin and negative for the pericyte markers Platelet-derived growth factor receptor beta (PDGFR- β) and Smooth Muscle Actin alpha (α -SMA) (Figure 2A). In the pericyte monoculture condition, the cells seem to have migrated towards the angiogenic cocktail, without the formation of sprouts. The monoculture was positive for both PDGFR- β and α -SMA (Figure



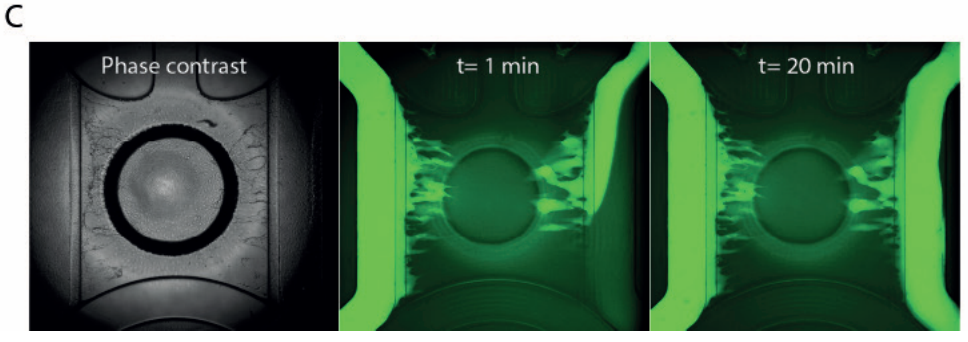


Figure 1 Endothelial microvessel culture and angiogenic sprouting. (A) The OrganoPlate Graft, based on a 384 well plate interface with 64 microfluidic chips integrated in the bottom, was used to assess angiogenesis. Endothelial vessels were formed on both sides of the chip, and sprouting was initiated with the addition of an angiogenic cocktail, which forms a gradient towards the endothelial vessel. **(B)** Phase contrast images of HUVECs sprouting towards an angiogenic cocktail over the course of 96 hours. Bottom left: zoom of the 96 h timepoint (zoom from white square of 96 h timepoint). Bottom right: immunofluorescent image of the same site as the bottom left. **(C)** A fluorescent dye was perfused through the left-lateral perfusion lane, and fluorescent were captured over time to visualize the perfusability of the vascular bed.

2B). Interestingly, we noticed that the pericytes located near the center of the chip stained predominantly more positive for α -SMA, and the pericytes located on the lateral side of the chip stained predominantly positive for PDGFR- β . When HUVECs and pericytes were co-cultured, angiogenic sprouts were observed after application of the angiogenic gradient (Figure 2C). Interestingly, α -SMA positive pericytes were found alongside the angiogenic sprouts.

Immunostaining revealed a complex network of sprouts, interacting and branching, but also growing over and under each other (Figure 1B, bottom right panel and Figure 3B). To accurately quantify the characteristics of this complex network, it is not sufficient to only image two-dimensional image data (as shown in Figure 1B and C), but to acquire and visualize the whole network in three dimensions.

High-throughput 3-dimensional vascular bed quantification

To study the vascular bed properties more precisely, we aimed to set up a method of quantifying the angiogenic sprouts in three dimensions. For optimization of the quantification method, a dataset was generated of vascular beds that sprouted for different durations ranging from 0 hours till 96 hours (Figure 3A). A rapid population of the graft chamber was observed with elongating angiogenic sprouts in till 72 hours after application of the cocktail, where in the period from 72 hours till 96 hours the sprouts seemed to start widening. A rapid and significant increase in the number of nuclei was found in the sprouting area from day 1 till day 4 quantified from a 2 dimensional maximum projection (Figure 3C, quantified from a maximum projection).

Subsequently, a workflow was developed to automatically combine and post process the z-images of the vascular bed (Figure 3B), to extract metrics such as sprout number and volume. The 3-dimensional quantification showed a similar trend, where the number of objects detected (Figure 3D) and the total volume in the angiogenic sprouts (Figure 3E) increased over time. Interestingly, the number

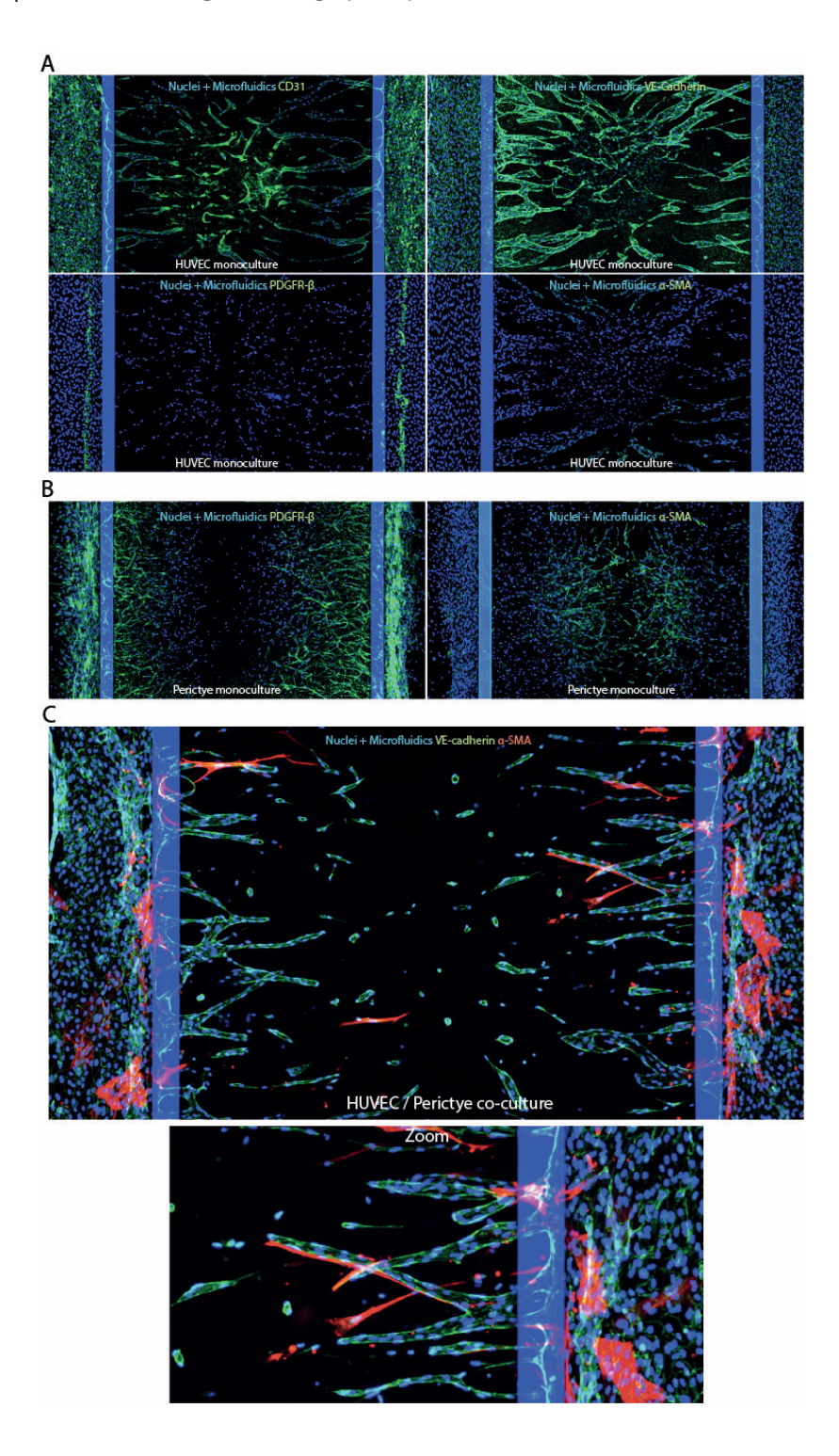


Figure 2 Immunofluorescent characterization of HUVEC monoculture and HUVEC/Pericyte co-culture in the OrganoPlate Graft after 4 days of sprouting. (A) Immunostaining of the HUVEC monoculture for various markers. The PhaseGuide are autofluorescent (blue lines), separating the center gel chamber from the adjacent perfusion lanes in the image. (B) Immunostaining of the pericyte monoculture. (C) Immunostaining of the HUVEC/Pericyte co-culture.

of objects detected from the 3 dimensional image did not increase from day 3 compared to day 4, where the total volume still increased.

Influence of withdrawal of growth factors on the pericyte-HUVEC co-culture

As a proof-of-concept, the newly developed imaging quantification method was assessed on the feasibility of angiogenesis inhibition studies. The inhibition of angiogenesis is an important focus in cancer therapy, and having a robust quantification method of angiogenesis inhibition would benefit drug development.¹⁸ To this end, our optimized HUVEC monoculture and HUVEC/pericyte co-culture was cultured, parts of our angiogenic sprouting cocktail were withdrawn to assess the effect on vascular bed formation (Figure 4A). No obvious difference was observed between the HUVEC monoculture and the HUVEC + pericyte co-culture condition. With the withdrawal of the complete cocktail, sprouts did not form in both monoculture and co-culture. Withdrawal of Sphingosine 1-phosphate (S1P) led to a visible regressed vascular bed formation in both monoculture and co-culture. Withdrawal of VEGF leads to a minor regression in vascular bed formation in both cultures.

After visual observation, our findings were confirmed with both our 2-D and 3-D quantification method (Figure 4B-D). Both quantification methods did not show a significant difference between the HUVEC monoculture and the co-culture conditions. A reduction in metrics was observed in the S1P and total sprouting mix withdrawal condition. In the 2D images (Figure 4B), 55% less nuclei were detected when S1P was withdrawn from the sprouting cocktail, where 75% less objects were detected in the 3D quantification (Figure 4C) in the HUVEC monoculture condition. When pericytes were added in the culture, these reductions changed to 65% and 68% respectively. Withdrawal of VEGF from the sprouting mix a 10%

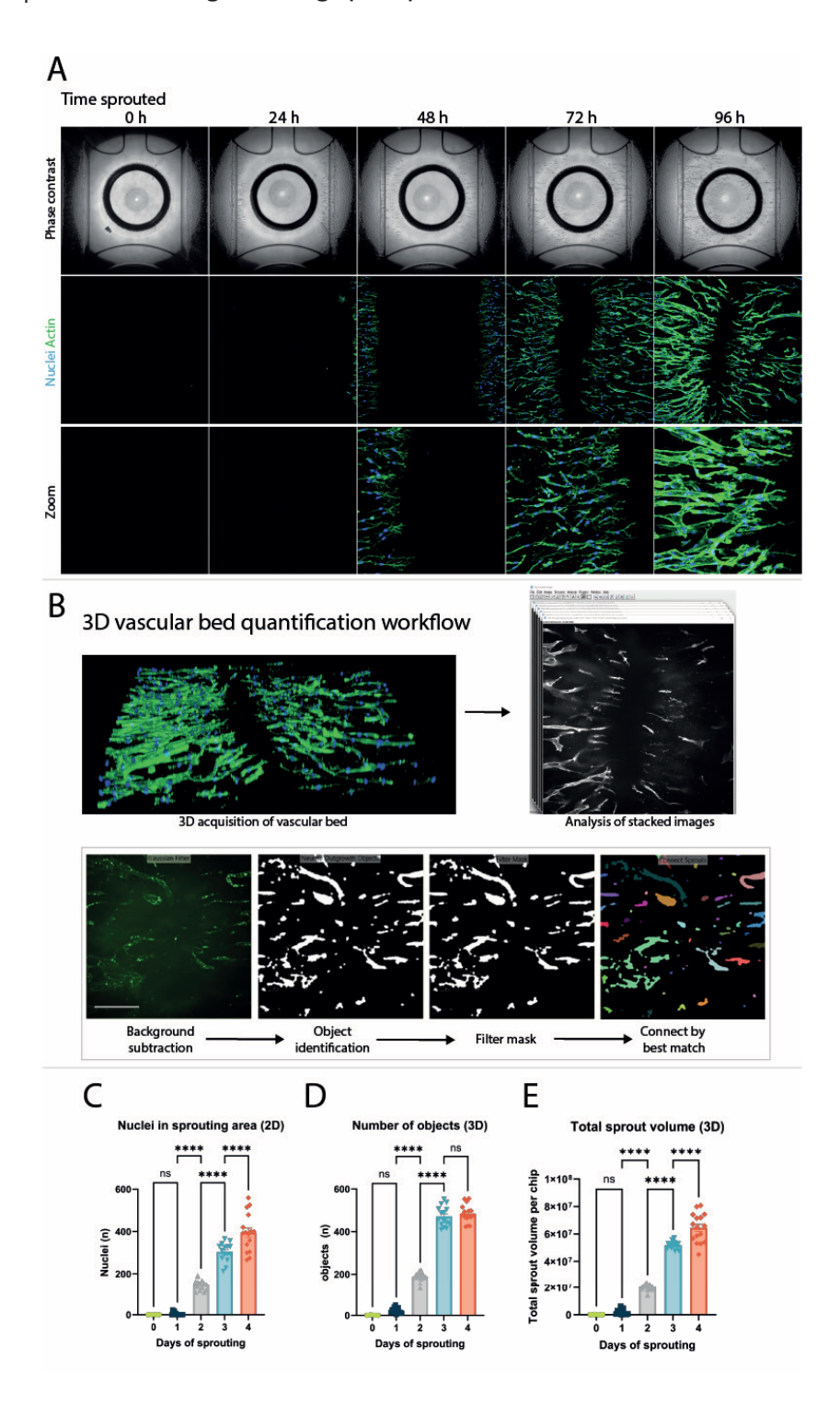


Figure 3 High-throughput 3-dimensional vascular bed quantification in HUVEC monoculture (A) Phase contrast (top) and immunofluorescent (middle and bottom) images of an angiogenesis induced vascular bed at different time points. **(B)** Workflow for the quantification of vascular beds in 3D. **(C-E)** Quantification of the vascular beds for number of nuclei in 2D **(C)**, number of detected objects in 3D **(D)** and total volume of the sprouts 3D **(E)**. Significance is calculated with an ordinary one-way ANOVA (Šídák's multiple comparisons test, ns = not significant, * p < 0.05, ** p < 0.01, *** p < 0.001, **** p < 0.0001, n=4 for day 0 condition and n = 14-16 chips for day 1-4 conditions)

reduction of total sprout volume was observed (Figure 4D) in the monoculture HUVEC and a 36% reduction in the co-culture HUVEC/Pericyte. This difference was also not significant. Interestingly, we found that the standard deviation of the measurements for the 'number of objects' metrics was lower than the other metrics, an average coefficient of variation (CV) was calculated of 24% for the total objects metric (3D imaging), whereas CV of 29% and 31% were calculated for the sprout volume (3D imaging) and nuclei (2D imaging) metrics, respectively.

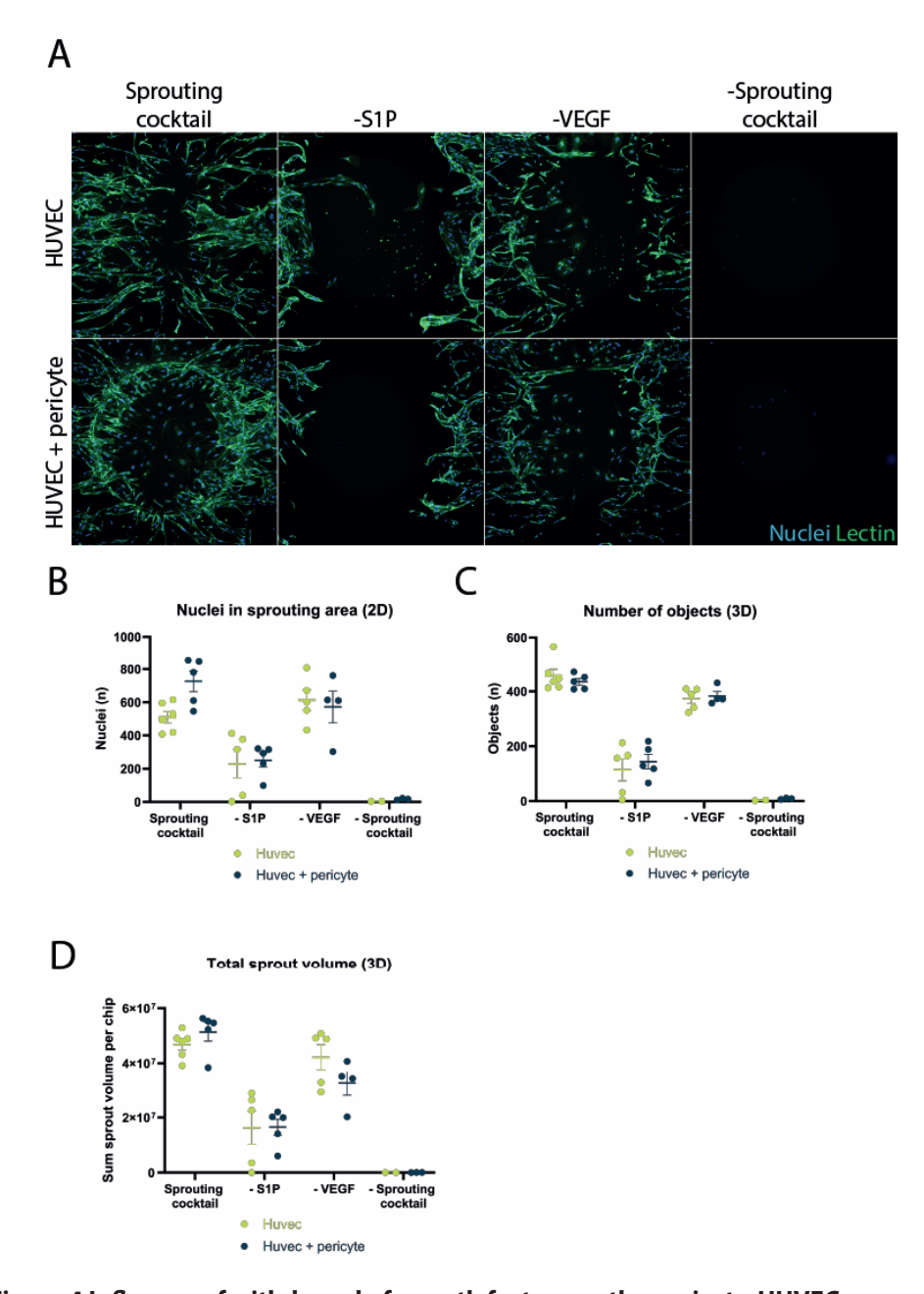


Figure 4 Influence of withdrawal of growth factors on the pericyte-HUVEC coculture (A) Immunofluorescent images of sprouted vascular beds with the sprouting cocktail added or (partly) withdrawn. (B-D) Quantification of the vascular beds for number of nuclei (2D) (B), number of detected objects (3D) (C) and total volume of the sprouts (3D) (D), n=3-6

Discussion

To capture the full properties of a complex three-dimensional structure such as a vascular bed, conventional 2D imaging and analysis, although more straightforward to automate, may not capture the full properties of the three dimensional structure. Our study strives to overcome these limitations by leveraging an innovative methodology, capable of automating the quantification of up to 64 vascular beds in a single session.

While similar methodologies exist for 2D in vitro cultures^{19,20} or in vivo,²¹ our approach of quantification of in vitro 3D angiogenic sprouts is unprecedented. Readouts were optimized to measure the number of objects and the total volume of sprouts in 3D, and compared this to a more general 2D quantification method (the total amount of nuclei present in the sample).

Interestingly, our comparison with conventional 2D quantification - based on the total amount of nuclei present in the sample - did not reveal significant differences, either in terms of vascular bed development or response to the withdrawal of growth factors from the sprouting mix. This result suggests that the information obtained from 2D and 3D quantification methods are complementary, providing a more comprehensive view of angiogenesis. Our study, however, highlighted an advantage of the 3D quantification approach: precision. Although this needs to be confirmed in repeat experiments, having a more precise measurement means more consistent results across multiple studies can be obtained, increasing the reliability of our findings. This could allow us to further estimate the maturity of the vascular bed, which is important for the development of new drugs that affect angiogenesis, for example in cancer treatment.^{22,23}

The inclusion of pericytes in our system was initially expected to yield significant differences in vascular bed formation in the growth factor withdrawal experiment compared to the monoculture HUVEC condition. Contrary to our expectations, no notable differences were observed, which could be attributed to a relatively short

culture duration to observe anastomosis of the sprouted vessels. Anastomosis plays a crucial role in vascular stabilization, with poorly or non-perfusable vessels being eliminated (pruning), while perfusable vessels get stabilized.²⁴

Looking ahead, our model could be further improved by extending our timelines to more thoroughly investigate the impact of pericytes on vascular stabilization post-anastomosis. Moreover, we intend to explore the potential role of pericytes in vasculogenesis, a process integral to vascular system development during embryonic stages and adult tissue repair and regeneration (Velazquez 2007). An additional optimization that could be undertaken involves the optimization of our 3D readout. In our study, we limited our examination to two descriptors of the vascular bed, recognizing that our readouts could be enhanced by incorporating additional descriptors like branching points into our model. Evaluating branching points is a critical aspect in the study of tumor angiogenesis, making their inclusion imperative for our model, especially if the aim is to broaden its applicability for the investigation of anti-cancer drugs.²⁵

In conclusion, our research provides a robust and innovative approach for quantifying a vascular bed in the OrganoPlate Graft. Alterations were tracked over time in sprout numbers under various conditions, thus facilitating high-throughput compound screening. The readout was compared to conventional two-dimensional quantification, and where similar observations in both readouts were made, the three-dimensional readout was found to be more precise. This readout establishes a solid base for future research aimed at optimizing in vitro angiogenesis study. By being able to quantify up to 64 vascular beds in 1 session, this opens the door to high-throughput compound screening.

References

- 1. Ouarné, M., Pena, A. & Franco, C. A. From remodeling to quiescence: The transformation of the vascular network. Cells and Development 168, (2021).
- 2. Rodriguez-iturbe, B., Pons, H. & Johnson, R. J. RÓLE OF THE IMMUNE SYSTEM IN HYPERTENSION. Physiol Rev 97, 1127–1164 (2022).
- 3. Betsholtz, C. Review Pericytes: Developmental, Physiological, and Pathological

- Perspectives, Problems, and Promises. (2011) doi:10.1016/j.devcel.2011.07.001.
- 4. Armulik, A., Abramsson, A. & Betsholtz, C. Endothelial/pericyte interactions. Circ Res 97, 512–523 (2005).
- 5. Gerhardt, H. & Betsholtz, C. Endothelial-pericyte interactions in angiogenesis. Cell Tissue Res 314, 15–23 (2003).
- 6. Viallard, C. & Larrive, B. Tumor angiogenesis and vascular normalization: alternative therapeutic targets. 409–426 (2017) doi:10.1007/s10456-017-9562-9.
- 7. Velnar, T. & Gradisnik, L. Tissue Augmentation in Wound Healing: the Role of Endothelial and Epithelial Cells. 72, 444–448 (2018).
- 8. Payne, L. B. et al. The pericyte microenvironment during vascular development. Microcirculation vol. 26 Preprint at https://doi.org/10.1111/micc.12554 (2019).
- 9. Norrby, K. In vivo models of angiogenesis. JCMM 10, 588–612 (2006).
- 10. Cimpéan, A. M. & Raica, M. Historical Overview of In Vivo and In Vitro Angiogenesis Assays.
- 11. Ponce, M. L. Tube formation: an in vitro matrigel angiogenesis assay. Methods Mol Biol 467, 183–188 (2009).
- 12. Heiss, M. et al. Endothelial cell spheroids as a versatile tool to study angiogenesis in vitro. The FASEB Journal 29, 3076–3084 (2015).
- 13. Rennie, M. Y., Whiteley, K. J., Kulandavelu, S., Adamson, S. L. & Sled, J. G. 3D Visualisation and Quantification by Microcomputed Tomography of Late Gestational Changes in the Arterial and Venous Feto-Placental Vasculature of the Mouse. Placenta 28, 833–840 (2007).
- 14. Dockery, P. & Fraher, J. The quantification of vascular beds: A stereological approach. Exp Mol Pathol 82, 110–120 (2007).
- 15. Lederlin, M. et al. Coronary imaging techniques with emphasis on CT and MRI. Pediatr Radiol 41, 1516–1525 (2011).
- 16. van Duinen, V. et al. Robust and scalable angiogenesis assay of perfused 3D human ipsc-derived endothelium for anti-angiogenic drug screening. Int J Mol Sci 21, 1–9 (2020).
- 17. Bonanini, F. et al. In vitro grafting of hepatic spheroids and organoids on a microfluidic vascular bed. Angiogenesis 25, 455–470 (2022).
- 18. El-Kenawi, A. E. & El-Remessy, A. B. Angiogenesis inhibitors in cancer therapy: Mechanistic perspective on classification and treatment rationales. Br J Pharmacol 170, 712–729 (2013).
- 19. Evensen, L., Micklem, D. R., Link, W. & Lorens, J. B. A novel imaging-based high-throughput screening approach to anti-angiogenic drug discovery. Cytometry Part A 77, 41–51 (2010).
- 20. Niemistö, A., Dunmire, V., Yli-Harja, O., Zhang, W. & Shmulevich, I. Robust quantification of in vitro angiogenesis through image analysis. IEEE Trans Med Imaging 24, 549–553 (2005).
- 21. Liu, M., Xie, S. & Zhou, J. Use of Animal Models for the Imaging and Quantification of Angiogenesis. (2018).
- 22. Vafopoulou, P. & Kourti, M. Anti-angiogenic drugs in cancer therapeutics: A review of the latest preclinical and clinical studies of anti-angiogenic agents with anticancer potential. Journal of Cancer Metastasis and Treatment vol. 8 Preprint at https://doi.org/10.20517/2394-4722.2022.08 (2022).
- 23. Qi, S., Deng, S., Lian, Z. & Yu, K. Novel Drugs with High Efficacy against Tumor Angiogenesis. International Journal of Molecular Sciences vol. 23 Preprint at https://doi.org/10.3390/ijms23136934 (2022).
- 24. Campinho, P., Vilfan, A. & Vermot, J. Blood Flow Forces in Shaping the Vascular System: A Focus on Endothelial Cell Behavior. Frontiers in Physiology vol. 11 Preprint at https://doi.org/10.3389/fphys.2020.00552 (2020).
- 25. Seano, G. et al. Modeling human tumor angiogenesis in a three-dimensional culture system. (2013) doi:10.1182/blood-2012-08.